Theoretical and Applied Climatology (2023) 152:895–910
https://doi.org/10.1007/s00704-023-04432-1

RESEARCH

Spatial minimum temperature reconstruction over the last three centuries for eastern Nepal Himalaya based on tree rings of *Larix griffithiana*

Narayan P. Gaire[1] · Santosh K. Shah[2] · Bimal Sharma[3] · Nivedita Mehrotra[2] · Uday Kunwar Thapa[4,5] · Ze-Xin Fan[3] · Prakash Chandra Aryal[6] · Dinesh Raj Bhuju[7]

Received: 1 November 2022 / Accepted: 12 March 2023 / Published online: 25 March 2023
© The Author(s), under exclusive licence to Springer-Verlag GmbH Austria, part of Springer Nature 2023

Abstract

We reconstructed summer (June–September) minimum temperature for eastern Nepal over the past 288 years (1733–2020 CE), using a total tree-ring width chronology of Himalayan Larch (*Larix griffithiana* (Lindl. and Gord.)) from Kanchanjunga Conservation Area (KCA). This study is the first minimum temperature reconstruction for the eastern Himalaya region of Nepal. We examined the response of the Larix ring-width chronology to different climate variables including precipitation, and minimum, maximum and mean temperatures. Of all climatic variables, minimum temperature has the strongest correlation with tree-ring chronology. This response revealed that the growth of the *L. griffithiana* is limited by temperature-induced physiological behaviors during summer season. The reconstruction shows fluctuating warm and cool periods during the entire period and captures warming during recent decades. This increasing warming trend appears to be unprecedented in the context of the past 288 years. We observed short (2.5 years) and multidecadal (35, 43, 71 and 100 years) cyclicity, which suggests possible atmospheric teleconnection with the broader circulation system of Atlantic Multidecadal Oscillation (AMO). This possible teleconnection is further revealed in spatial field correlation and also supported by temporal comparison of the reconstruction with instrumental- and proxy-based AMO records.

Keywords Himalayan Larch · Kanchenjunga Conservation Area · Summer · Atlantic Multidecadal Oscillation · Volcanic eruptions

✉ Santosh K. Shah
santoshkumar_shah@bsip.res.in

1 Department of Environmental Science, Patan Multiple Campus, Tribhuvan University, Lalitpur 44700, Nepal

2 Birbal Sahni Institute of Palaeosciences, 53-University Road, Lucknow 226007, India

3 CAS Key Laboratory of Tropical Forest Ecology, Xishuangbanna Tropical Botanical Garden, Chinese Academy of Sciences, Menglun, Mengla 666303, Yunnan, China

4 Bren School of Environmental Science and Management, University of California Santa Barbara, Santa Barbara, CA, USA

5 Cooperative Programs for the Advancement of Earth System Science, University Corporation for Atmospheric Research, Boulder, CO, USA

6 GoldenGate International College, Battisputali, Kathmandu, Nepal

7 Nepal Academy of Science and Technology, Khumaltar, Lalitpur, Nepal

1 Introduction

The eastern Himalaya region covers a broad spectrum of ecological zones of eastern Nepal, northeastern regions of India, Bhutan, the Tibet and Yunnan of China, and northern Myanmar (Zurick et al. 2005; Sharma et al. 2010; Shrestha and Devkota 2010). The complex mountain topography of the region has created diverse bioclimatic zones such as near tropical, subtropical, lower temperate, upper temperate, subalpine evergreen, alpine evergreen, alpine shrubs and meadows, and is ecologically rich in natural and crop-related biodiversity (Sharma et al. 2010; Chaudhary et al. 2015). The Kangchenjunga Landscape (KL) in the eastern Himalaya geographically comprises a part of eastern Nepal, Sikkim and Darjeeling in India and western Bhutan. The KL is considered as one of the most biodiversity-rich landscapes in the eastern Himalaya region (Chettri et al. 2010), constituting many endemics, endangered and threatened flora and fauna (Chaudhary et al. 2015; ICIMOD 2015). The eastern Himalaya is not only the home for millions of human populations including many ethnic communities, but also a critical part of global biodiversity hotspot; it comprises parts of Himalayan Hotspot, Indo-Burma Hotspot, Mountains of Southwest China Hotspot, and 25 Global Ecoregions including Crisis Ecoregions, and Endemic Bird Areas (Myers et al. 2000; Olson and Dinerstein 2002; Brooks et al. 2006; Sharma et al. 2010). However, global climate change poses acute threats to biodiversity in this region (Dhar 2002; Chettri et al. 2010).

The KL region is warming rapidly with annual and seasonal temperature increasing at the rate of 0.01–0.015 °C/year (Chettri et al. 2010; Shrestha and Devkota 2010). The rate of warming is higher during winter (December–February) season (0.20–0.3 °C/year), with higher elevated mountainous regions experiencing greater magnitude of winter warming (Chettri et al. 2010). Observations show that the frequency and intensity of weather extremes are increasing along with increase in daily maximum and minimum temperatures by 0.1 °C and 0.3 °C per decade respectively over the period of 1975–2010 (Shrestha et al. 2017). Precipitation records do not demonstrate any consistent long-term trends but the frequency and amount of intense rainfall as well as the number of consecutive dry days have increased (Zhan et al. 2017; Shrestha et al. 2017). The increase in mean and extreme temperatures over the Himalayan region including eastern Himalayas of Nepal (Sun et al. 2017) has several biophysical and socioeconomic consequences. This rapid warming has accelerated snow and glacier retreat, increased glacial lake size, and reduced the permafrost-covered area (Asahi and Watanabe 2000; Fukui et al. 2007; Bolch et al. 2012; Chattopadhyay et al. 2016). In addition, phenological change of the organisms, alteration in the range and distributions of species are observed in various regions of eastern Himalaya (Shrestha et al. 2012; Telwala et al. 2013; Gaire et al. 2017; Sigdel et al. 2018). Warmer temperatures are also causing the trees growing at their vertical limits to advance upslope at the rate of 0.01 to 0.93 m/year (Chhetri and Cairns 2015; Gaire et al. 2017; Sigdel et al. 2018).

Understanding of long-term climate change and variability is required to assess long-term environmental changes. This shall in turn aid to make decisions on biodiversity conservation in the context of anthropogenic global warming in this critically important KL region. However, the instrumental observations of climate and hydrology in eastern Himalayan region are brief and are sparsely located, limiting our understanding of temperature and precipitation changes only over the past four decades. In order to extend climate records prior to the instrumental period, it is a common practice to use information preserved in natural archives including tree rings (Cook et al. 2010; Sano et al. 2013; Shah et al. 2014a; Krusic et al. 2015; Thapa et al. 2015).

Owing to its diverse climatic zones and deep elevation gradient, the KL region has many conifers and broad-leaved tree species that have potentials for dendroclimatic reconstructions. They are conifer taxa such as *Abies densa*, *A. spectabilis*, *Juniperus indica*, *J. recurva*, *Larix griffithiana*, *Picea spinulosa*, *Pinus kesiya*, *P. merkusii*, *P. roxburghii*, *P. wallichiana*, *Taxus baccata* and *Tsuga dumosa* (Bhattacharyya and Chaudhary 2003; Cook et al. 2003, 2010; Shah and Bhattacharyya 2012; Sano et al. 2013; Krusic et al. 2015; Shah et al. 2019). The known broad-leaved taxa such as *Betula utilis*, *Rhododendron campanulatum*, and *Toona ciliata* have been studied for dendroclimatic analysis (Liang et al. 2019; Panthi et al. 2021; Shah and Mehrotra 2017). However, compared to other parts of the greater Himalayas, very few dendroclimatic studies have been carried out in eastern Himalaya, and those are mostly from Indian (Shah et al. 2014a) and Bhutan Himalaya (Krusic et al. 2015). Chaudhary and Bhattacharyya (2000) studied tree-ring of *L. griffithiana* from the Arunachal Pradesh, eastern Indian Himalaya and indicated its potential for the reconstruction of summer temperature. Bhattacharyya and Chaudhary (2003) reconstructed late-summer (July–September) temperature for the eastern Indian Himalayan region using tree-ring data of *A. densa.* Shah et al (2014b) carried out stream flow reconstruction from north Sikkim using multiple tree-ring parameters of *L. griffithiana*. Sano et al. (2013) estimated more than 200 years of May–September precipitation using oxygen isotope ($\delta^{18}O$) measurements from tree rings of *J. indica*, *L. griffithii*, and *P. spinulosa* in the Bhutan Himalaya. Similarly, Krusic et al. (2015) used tree-ring chronology of *P. spinulosa* from Bhutan and produced the first multi-centennial (1376–2013 CE) summer (June–August) temperature reconstruction for the country. While significant advancement has been achieved in tree-ring reconstructions in central and western Nepal (Cook et al. 2003; Thapa et al. 2015; Bhandari et al. 2019; Liang et al. 2019; Aryal et al. 2020a; Gaire et al. 2020), no robust dendroclimatic reconstructions exist from eastern Nepal Himalaya including Kanchenjunga Conservation Area (KCA). However, attempts have been made to assess the regeneration, climatic sensitivity and dendroclimatic suitability of *L. griffithiana* from KCA, Langtang and Manaslu region (Bhatta et al. 2018; Aryal et al. 2020b). Therefore, in this study, we aim to (1) develop tree-ring site chronology of *L. griffithiana*, (2) assess the growth response of *Larix* to climate variables, and (3) reconstruct multi-centennial climate based on tree-ring width of *L. griffithiana*. In botanical nomenclature, *L. griffithiana* and *L. griffithii* are synonymously used.

2 Materials and methods

2.1 Study area and sample collection

The present study site is located in the Kanchenjunga Conservation Area (KCA) in east Nepal. The KCA is named after Mt. Kanchenjunga (8586 m), established in

1997 with an area of 2035 km^2 and included in IUCN's protected area management category IV. The KCA is an important area of the broader Kanchenjunga Landscape (KL), a trans-boundary landscape designed for the biodiversity conservation and resource management in Taplejung District of eastern Himalaya region of Nepal (DNPWC 2018). The KCA adjoins the Qomolangma National Nature Preserve in Tibet, China in the north, and the Khangchendzonga National Park/Biosphere Reserve in Sikkim, India in the east (Bhuju et al. 2007; Kandel et al. 2016; DNPWC 2018). It also falls within the Sacred Himalayan Landscape, which is developed by WWF Nepal in partnership with the International Centre for Integrated Mountain Development (Aryal et al. 2010). KCA has diverse forest vegetation viz., subtropical evergreen forest (800–1200 m), lower temperate forest also known as lower temperate mixed broadleaf forest (1200–2500 m), upper temperate forest also called upper temperate mixed forest or temperate cloud forest (2500–3500 m), sub-alpine zone (3500–3900 m) and alpine zone (3900–4600 m) (Carpenter et al. 1994; Bhuju et al. 2007; DNPWC 2018). Compared to other areas of eastern Nepal, evergreen broadleaf taxa in KCA grow towards the higher elevation regions in the valley of the Ghunsa Khola, with *Acer campbellii* the only abundant deciduous broadleaf tree (Carpenter et al. 1994). There are 4–5 conifer species growing in the same stand indicating the high species richness of conifers in this area. At higher elevations near Ghunsa Village (3300 to 3400 m a.s.l.), *A. spectabilis* replaces *T. dumosa* on stable slopes and old moraines to form a subalpine forest, while *L. griffithiana* forms pure stands on depositional terraces, loose slopes and other places prone to a higher rate of disturbance (Carpenter et al. 1994). The *Larix* forests of the region are ecologically significant because they represent the western most extreme for this unique, deciduous conifer of the eastern Nepal Himalaya (Carpenter et al. 1994). *L. griffithiana* is distributed in eastern Himalaya from East Nepal through Darjeeling, Sikkim, Bhutan, Arunachal Pradesh (India), NE Upper Burma (Myanmar), and Chumbi Valley in Tibet at 2400–3650 m and mostly growing on glacial moraine (Sahni 1990).

The tree-core sample collection was carried out in the Ghunsa Khola area, namely Phale and Ghunsa in field expedition carried out during April, 2014 and September–October, 2015 (Fig. 1). We collected tree-core samples from the least anthropogenically disturbed *L. griffithiana* dominated forest stands. The slope of the sampling site ranges from 20 to 30° and sampling site covers an elevation range from 3300 to 3600 m. Tree cores were collected using a Swedish Haglof increment borer following the commonly used technique (Fritts 1976; Cook and Kairiukstis 1990; Speer 2010). The cores were collected at breast height (~ 1.3 m) and two cores per tree were collected where possible. A total of 120 cores from 60 trees of *L. griffithiana* were collected for tree-ring analysis.

2.2 Tree-ring sample processing and chronology development

The collected tree-core samples of *L. griffithiana* were brought to the laboratory for preparation and measurement.

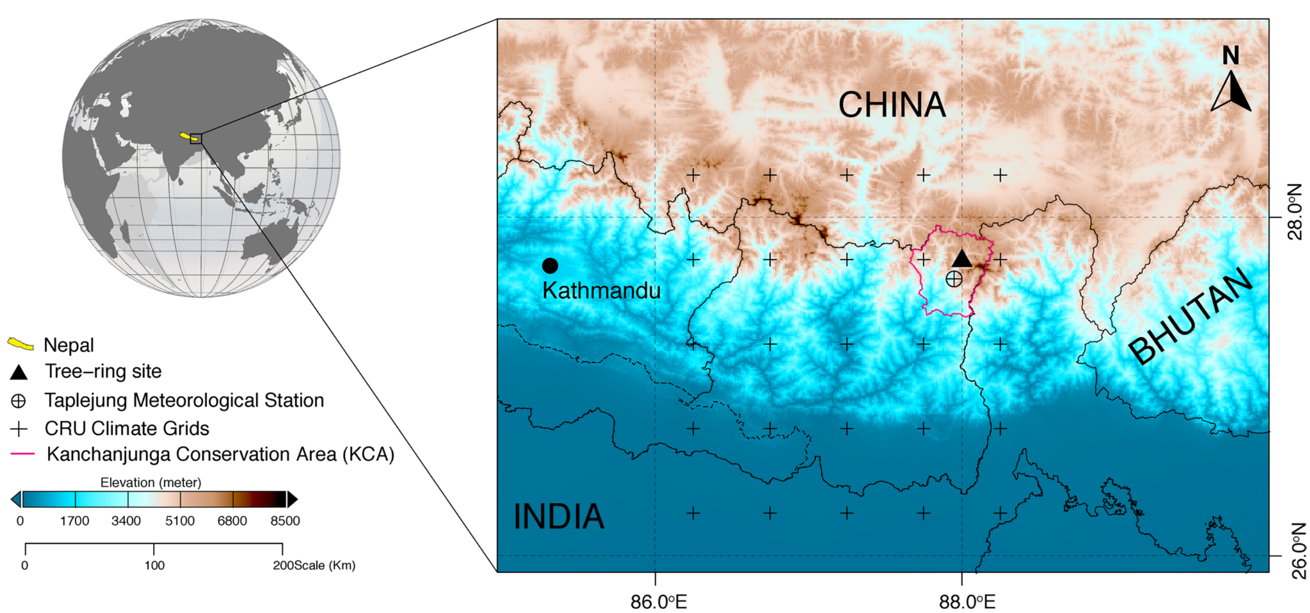

Fig. 1 Map showing the locations of tree-ring site of *Larix griffithiana* from Kanchanjunga Conservation Area, eastern Nepal Himalaya and meteorological station, Taplejung along with 25 grid points of gridded CRU climate data

The cores were mounted on wooden frames by using water soluble adhesive with the transverse surface of the core facing up. After air drying, cores were sanded and polished by a belt sander machine. Furthermore, manual sanding was done using successively finer grades of sand paper (600 to 1000 grits) until optimal surface resolution allowed annual rings to be visible under the microscope. Each annual rings were counted under a Leica stereo zoom microscope and assigned a calendar year with the help of the known date of formation of the outer rings validated by cross dating. The width of each ring was measured to the nearest 0.001 mm precision with the LINTAB^{TM5} measuring system attached to a computer using the TSAP-Win software (Rinn 2003). All tree-core samples were cross dated by matching patterns of relatively wide and narrow rings across the samples to account for the possibility of ring-growth anomalies such as missing rings, false rings, or measurement error (Fritts 1976). Each tree-ring width series was visually (using the math graphs) and statistically (using Gleichläufigkeit, *t*-values, and the cross-dating index, CDI) cross dated using the software package TSAP-Win (Rinn 2003). The accuracy of the cross dating of all tree-ring series was further checked using COFECHA (Holmes 1983). Those series which were young, showed irregular growth pattern, had several breakages, had very low correlation with master series in TSAP or in COFECHA were discarded and not included in tree-ring chronology development.

In order to remove the geometric and ecological growth trends largely unrelated to climate, and to remove effects of differential mean growth rates among individual trees prior to averaging into the mean chronology (Cook 1985; Cook and Kairiukstis 1990), standardization of each series was carried out. The standardization of each tree-ring width series was done by fitting a negative exponential growth curve and then dividing the measured value by the curve value at each year in RCSSigFree programs (Melvin and Briffa 2008). The standardization method in this program generates a series of detrending curves that are free of growth patterns common to all measurement series, and preserves low to medium frequency signal in the final chronology (Melvin and Briffa 2008)**.** The individual detrended series were averaged using a bi-weight robust mean function (Cook 1985; Cook and Kairiukstis 1990) to produce the mean chronology. The average correlation between series (RBAR) and the expressed population signal (EPS) (Wigley et al. 1984), which are considered as measures of common signal strength of chronologies were calculated in a running window of 50 years. The EPS is an indication of how well the site chronology estimates the population chronology. The value of 0.85 was taken as a threshold to judge the reliable portion of the chronology time series captured by adequate sample depth (Wigley et al. 1984). Furthermore, various chronology statistics (Fritts 1976; Speer 2010) were calculated for stabilized signal-free chronology for full and common periods having maximum samples.

2.3 Climate data

The KCA region has been largely dominated by monsoon climate; however, in the northern corner of the area, many dry valleys also exist (Böhner et al. 2015). We use climate date from Taplejung meteorological station (27.35° N Latitude, 87.66° E Longitude, 1732 m), which is the nearest meteorological station from our present tree-ring sampling site (Fig. 1). This station records both temperature and precipitation datasets. This station showed, winter (December–February), spring (March–May), summer (June–September) and autumn (October–November) receive 2.6, 20.7, 71.8, and 4.9% of annual precipitation, respectively. During 1948–2013 CE, the average annual total precipitation was 1981 mm (Fig. 2). The highest annual precipitation (2505 mm) was recorded in 2003 while the lowest (1408.9 mm) was recorded in 2009. There is a slight increase in annual precipitation by a rate of 0.84 mm/yr, but it is statistically not significant. The average mean annual temperature for 1962–2012 was 16.2 °C (Fig. 2). January and August are the coldest and warmest months in the area, with lowest temperature recorded in January 1983 (2.4 °C) and highest in August 2012 (26.8 °C). During 1962–2013, the mean annual temperature has increased by 0.023 °C/year with a more pronounced increase in average annual maximum temperature (0.034 °C/year) as compared to minimum temperature (0.01 °C/year). In addition to instrumental record, gridded climate data from Climate Research Unit (CRU) covering the sampling area were also used (Harris et al. 2020). We extracted monthly minimum (TMN), maximum (TMX) and mean (TMP) temperature and precipitation datasets for 25 grid points covering 26.55–28.25° N and 86.25–88.25° E to represent regional climate (Fig. 1). The correlations between annual mean temperature of Taplejung with each 25 CRU temperature grids points range from 0.775 to 0.838 ($p < 0.0001$). However, we have not observed significant positive correlation between gridded and station-based precipitation, which is common for topographically varied region such as KL. Similar to instrumental record from Taplejung station, CRU gridded data also exhibited positive trends in TMP, TMX, and TMN, with higher magnitude of warming in the period common to instrumental data (1962–2013 CE).

2.4 Response of tree growth to climate

Longer climatic data from near the tree-ring sampling site is more reasonable to examine the response of tree growth to climate. Taplejung is the nearest meteorological station located about 40 km from our sampling site. However, the length of temperature records is shorter compared to precipitation data. In addition, both climatic variables have

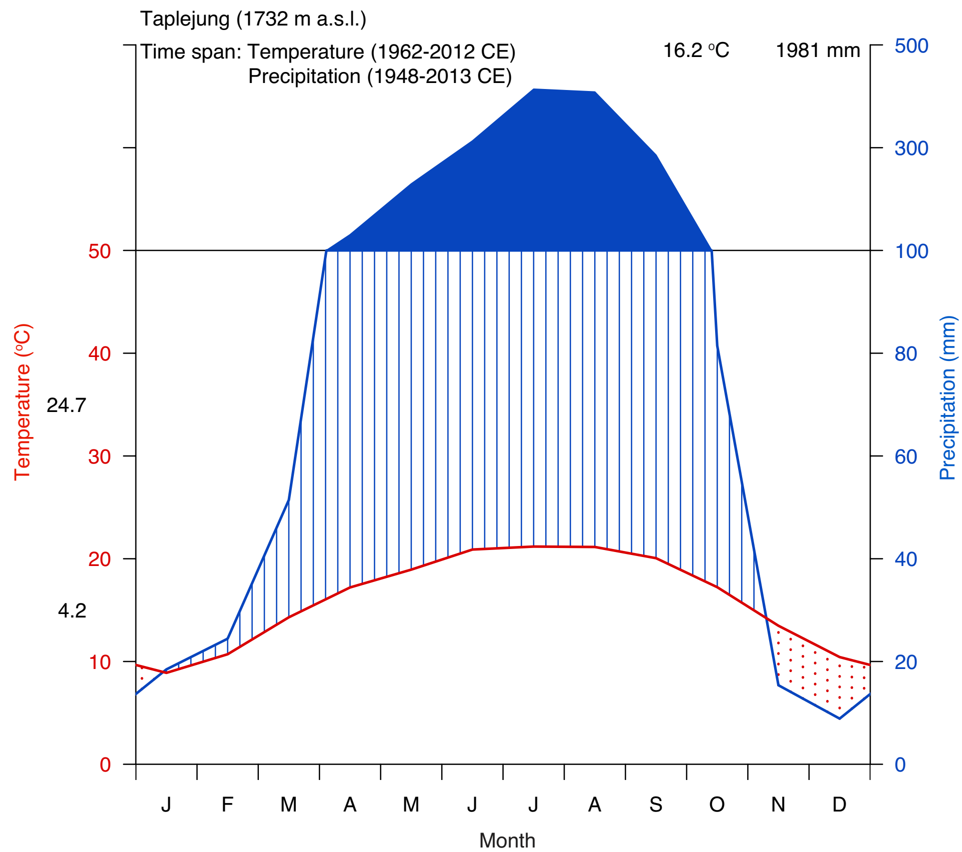

Fig. 2 Walter and Leith climate diagram of the Taplejung meteorological station. The blue line represents monthly precipitation (for 1948–2013 CE) and red line represent monthly temperature (for 1962–2012 CE). The monthly mean maximum of the warmest month (August) is 24.7 °C and the monthly mean minimum temperature is 4.2 °C for January. The upper right corner of the diagram shows the mean annual temperature (16.2 °C) and total annual precipitation (1981 mm). The blue filled area represents wet period and the red dotted area represents dry period

some missing records (precipitation, 7% and temperature 6.2%). Alternatively, we used gridded CRU climate datasets to establish tree-growth climate relationship and to establish regional climate response. The spatial field correlations between our tree-ring chronology of *L. griffithiana* and CRU climate variables for all the 25 grids were calculated for a 14-month dendroclimatic window starting from September of the prior year through the current year October. Based on the overall spatial correlation analysis, the seasonal climate which strongly limits the growth of *L. griffithiana* has been selected for climate reconstruction using modified point-by-point regression methodology.

2.5 Palaeoclimate reconstruction and teleconnections

The climate variable with strongest and significant association with *L. griffithiana* chronology was reconstructed using a modified version of the point-by-point regression (PPR) method (Cook et al. 2010, 2015). The PPR method has been widely used for climate field reconstructions based on either single or multiple tree rings datasets (Cook et al. 1999, 2004, 2010, 2015). The PPR methodology can be used as a flexible procedure in small-scale experiments with single predictor (a tree-ring chronology) and a single predictand (a climate record). When PPR method is used with a single predictor and predictand, it estimates a simple linear regression model that transforms the tree-ring time series into the climate time series (Krusic et al. 2015). The AR models were estimated from the calibration period data and applied back in time over the lengths of the tree-ring and climate data not used for calibration. This produces approximate 'white noise' reconstructions which is later 'reddened' by adding the AR persistence in the instrumental data and applied for full lengths of the reconstructions.

The time stability of the PPR model was tested by using rigorous calibration and validation tests commonly used in tree-ring–based climate reconstructions using PPR methodology (Cook et al. 1999, 2004, 2010, 2015). The calibration statistics used are the coefficient of determination (CRSQ) and cross-validation reduction of error (CVRE). The CVRE is calculated using 'leave-one-out' procedure and considered as analogous to R^2 based on Allen's PRESS statistic (Allen 1974). The CVRE is considered as a more traditional measure of explained variance than CRSQ (Cook et al. 2015). The validation period statistics considered are the Pearson correlation coefficient squared (VRSQ), the reduction of error statistic (VRE) and the coefficient of efficiency (VCE). The VRSQ should be positive at the 95% level to judge the significant reconstruction skill. In case of VRE and VCE, there are no theoretical significance tests available; however, if VRE and VCE value is greater than 0, then the reconstruction has some skill in excess of the calibration or verification period means (Cook et al. 1999, 2010, 2015). Once the PPR method based on linear regression model was considered effective and stable, it was used to reconstruct our target significant climatic variable. The final reconstruction was truncated to the effective chronology period based on commonly used EPS threshold criteria, i.e., > 0.85 (Wigley et al. 1984).

Furthermore, the reconstruction was compared with independent proxy-based summer temperature records from the adjoining regions. Additionally, we also performed spatial correlations between our reconstruction and global Sea Surface Temperature (SST) datasets to assess the coherency and atmospheric teleconnection patterns. For this purpose, two different SST datasets viz., Hadley Centre Sea Ice Sea Surface Temperature (HadISST, Rayner et al. 2003) and NOAA Extended Reconstructed Sea Surface Temperature version 5 (ERSST v5, Huang et al. 2017) were used. The spatial field correlations analysis was performed in the KNMI Climate Explorer (Trouet and Oldenborgh 2013; http://climexp.knmi.nl/). The Power spectral analysis using the Multiple-Taper Method (MTM, Mann and Lees 1996) was applied on reconstruction to compute the periodicity in the time series. The localized variation of power to identify domain periods within reconstructed variable was assessed using wavelet analysis (Torrence and Compo 1998).

3 Results and Discussion

3.1 Assessment of tree-ring chronology of *L. griffithiana*

The tree-core samples have distinct ring boundary with a clear demarcation from earlywood to latewood. Based on the well cross dated samples the *L. griffithiana*, a 292-year long ring-width chronology (1724–2015 CE) was developed (Fig. 3). The chronology statistics revealed that it has good dendroclimatic potential with moderate mean sensitivity (1.01), high standard deviation (0.179). The common period (1958–2008 CE) Rbar statistics observed between all series, within trees and between trees are 0.499, 0.692 and 0.497 respectively and are higher and significant. The EPS of the site chronology was above (0.982) the threshold limit of 0.85 (Wigley et al. 1984) and the running EPS showed that the chronology is reliable till 1733 (Fig. 3). The signal to noise ratio and variance explained in the first principal component analysis are 55.9 and 52.9% respectively, which showed that common climatic factor affects the growth of the trees in the study site.

The tree-ring chronology statistics observed in the present study are comparable to those reported for the same or other conifer species from different parts of the eastern Himalaya (Bhattacharyya et al. 1992; Chaudhary and Bhattacharyya 2002; Cook et al. 2003; Shah and Bhattacharyya 2012; Shah et al. 2014b; Krusic et al. 2015; Thapa et al. 2017). The chronology exhibits growth fluctuations over time with positive growth during the first half of twentieth

Fig. 3 Tree-ring chronology of *Larix griffithiana* from eastern Nepal Himalaya region along with sample size, EPS and RBAR

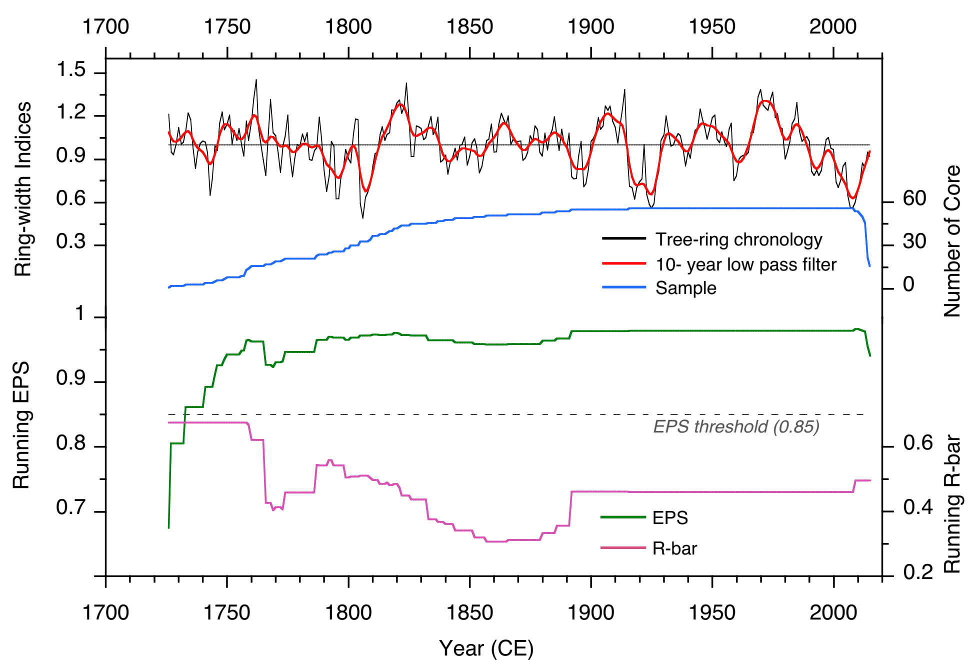

century followed by continuous growth decline in the recent few decades (after 1970s) (Fig. 3). The Larix chronology displayed reduced growth during dry periods and enhanced growth during warm and moist periods, suggesting that Larix trees in eastern Himalaya are sensitive to climatic variations. The observed long-term growth trend is almost similar with that in the composite chronology developed for the Bhutan Himalaya (Krusic et al. 2015). Other studies have also observed similar growth trends with twentieth century growth enhancement in different regions in the Himalaya (Krusic et al. 2015; Gaire et al. 2020). A positive growth trend was observed in the nationwide composite chronology of Nepal (Thapa et al. 2017). But we observed growth decline in our chronology in the recent decades, which suggests that growth trends might vary regionally and accordingly in tree species. Larix species was not included in the country-wise tree growth synthesis by Thapa et al. (2017). A decline in growth trend was also observed in tree-ring studies carried out in *B. utilis* from central Nepal (Tiwari et al. 2017) and in *A. spectablis* and *B. utilis* from western Nepal (Bista et al. 2021).

3.2 Regional response of climate on tree growth of *L. griffithiana*

The growth-climate response analysis using field correlations shows negative relationship between the growth of *L. griffithiana* and temperature during most of the months. The Larix chronology has the strongest correlation with June–September minimum temperature ($JJAS_{TMN}$) compared to maximum and mean JJAS temperatures across the 25 CRU grid points (Fig. 4). There is no significant correlation between tree growth and precipitation. The limited ecological distribution of this species at an altitude of 2400–3650 m a.s.l. in the eastern Himalaya where it grows on glacial moraines on well-drained soils of grassy slopes (Ostenfeld & Larsen 1930; Sahni 1990) distinguishes its preferences of lower temperature zones and moisture availability. The species growth consequently can be impacted due to lack of moisture and variations in minimum temperature.

The positive relationship with precipitation and negative with temperature during summer and late summer season indicates that moisture availability during the beginning or whole growing season is the primary limiting factor to the Larix growth.

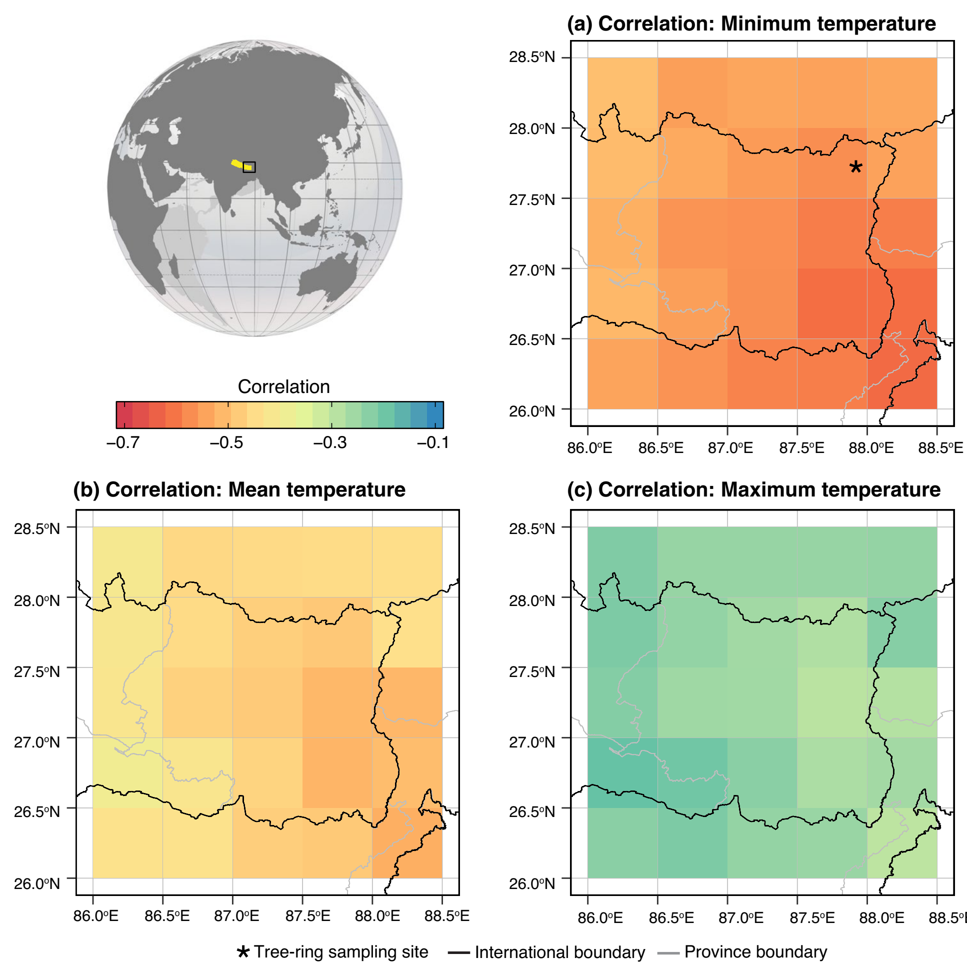

Fig. 4 Spatial correlation between tree-ring chronology of *Larix griffithiana* and **a** minimum **b** mean and **c** maximum temperature for 1951–2015 CE

Larix is a deciduous conifer species, optimum climatic conditions are therefore very important for the species to attain optimum growth. Compared to other species and regions, very few dendroclimatic studies have been carried out from the eastern Himalaya to adequately weigh the climate response of our Larix chronology from others. Earlier studies also showed that the growth of this tree is influenced by summer to late summer temperature in the eastern Himalaya region (Chaudhary and Bhattacharyya 2000; Yadava et al. 2015). This growth response is typical for most conifer tree-ring chronologies from the dry mountain valleys in the Himalaya (Chaudhary and Bhattacharyya 2000; Bhattacharyya and Chaudhary 2003; Cook et al. 2003; Gaire et al. 2014; Yadava et al. 2015). The *L. griffithiana* growing in Arunachal Pradesh, eastern Himalaya exhibited a higher growth in relation to increased temperature during November of the previous year and May and July of the current growth year, whereas it displayed negative relationship current January temperature (Chaudhary & Bhattacharyya 2000). But in the present study, warm summer temperature still has a negative influence on the Larix growth. In Arunachal Pradesh region, precipitations during August and September of the previous year and July of the current year have inverse relationships with tree growth, whereas January and February of the current year exhibit a direct relationship with growth (Chaudhary & Bhattacharyya 2000). Differing from our findings, the *L. chinensis* from Qinling Mountains in China showed a positive relationship with summer temperature (Liu et al. 2018). These differences in the response might be associated with the differences in the topography in India and Nepal Himalaya and China. Similar to our results, tree-ring analysis from *A. densa* growing at the tree line in the Sikkim (east of the present sampling site) and Arunachal Pradesh from eastern Himalaya region shows negative relationship between the temperatures during the current year's summer months (Bhattacharyya and Chaudhary 2003). The tree-ring network-based studies from Nepal Himalaya (Cook et al. 2003) also obtained negative response with summer temperature in some sites. In dry Himalayan valleys, the higher temperature during late-spring and summer months leads to more evaporative water demand causing shortage of water for photosynthesis and tree growth, since temperature during these periods often would be high. Several possible reasons why trees from different parts of Himalaya have negative response to summer temperature have been explained in several studies (Chaudhary & Bhattacharyya, 2000; Bhattacharyya and Chaudhary 2003; Cook et al. 2003; Yadav et al. 2004; Gaire et al. 2014; Yadava et al. 2015).

3.3 JJAS Minimum temperature ($JJAS_{TMN}$) reconstruction

Based on the correlation result, we selected June–September minimum temperature ($JJAS_{TMN}$) as a target variable for reconstruction. For this tree-ring chronology of *L. griffithiana* as the predictor and the average June–September minimum temperature ($JJAS_{TMN}$) based on the 25 CRU grid points as predictand. The correlation was carried out as 1-tailed test using negative correlations. The tree-ring (t and t + 1) and instrumental $JJAS_{TMN}$ data used for calibration were pre-whitened using autoregressive (AR) models fit to correct for differences in autocorrelation between them (Cook et al. 1999; Meko 1981). We developed robust spatial reconstruction model between the tree-ring chronology of *L. griffithiana* and average $JJAS_{TMN}$ for each 25 CRU grid points. The calibration period of 1975–2014 CE (40 years) was reserved for the calibration analysis and $JJAS_{TMN}$ records from 1951 to 1974 (24 years) was withheld from the calibration period to test validation skill of estimated $JJAS_{TMN}$. Additionally, the reconstruction was updated up to the last year (2020 CE) of instrumental datasets using 'composite-plus-scale' (CPS) method (Smerdon et al. 2015). Both CRSQ and VRSQ statistics for all the 25 grid points are statistically significant (Fig. 5). Except VCE for two grid points, all other three statistics, calibration (CVRE) and validation statistics (VRE and VCE) are found positive and therefore the reconstruction model is reliable for all the CRU 25 grid points (Fig. 5). We further modelled the tree-ring chronology of *L. griffithiana* against the average $JJAS_{TMN}$ across 25 grid points. This final model explains 36.4% of variations in instrumental $JJAS_{TMN}$ during calibration period of 1975–2014 CE. Using this model, 283 years long (1733–2015 CE) average $JJAS_{TMN}$ was reconstructed for the eastern Nepal Himalaya region (Fig. 6). The average $JJAS_{TMN}$ reconstruction model has robust skill based on the calibration verification statistics. The calibration period CRSQ and CVRE are 0.364 and 0.284, respectively. The verification period VRSQ, VRE and VCE are 0.422, 0.665 and 0.273, respectively.

3.4 Assessments of $JJAS_{TMN}$ reconstruction

Our $JJAS_{TMN}$ reconstruction shows an overall increase in the temperature with unprecedented late twentieth century warming. The observed warming trend in our reconstruction is similar to other tree-ring–based temperature reconstructions from the Himalaya (Cook et al. 2003; Krusic et al. 2015; Aryal et al. 2020a; Gaire et al. 2020). The early eighteenth century cooling and warming from the late nineteenth century until the present in our reconstruction are consistent with other summer temperature reconstructions for Nepal, Bhutan, India, Tibetan Plateau, as well as with large-scale continental-scale reconstructions from south and east Asia (Cook et al. 2003; Krusic et al. 2015; Yadava et al. 2015; Cook et al. 2015; PAGES2k 2013; Wang et al. 2015) (Fig. 7). Our reconstruction shows a relatively longer cooling episode during 1810–1822 that coincides with two major Indonesian volcanic eruptions; 1809 unknown and 1815 Tambora (Cole-Dai et al. 1997; Stothers 1984). These explosive eruptions, specifically Tambora, are among the largest eruptions over the Common Era (Gao et al. 2008;

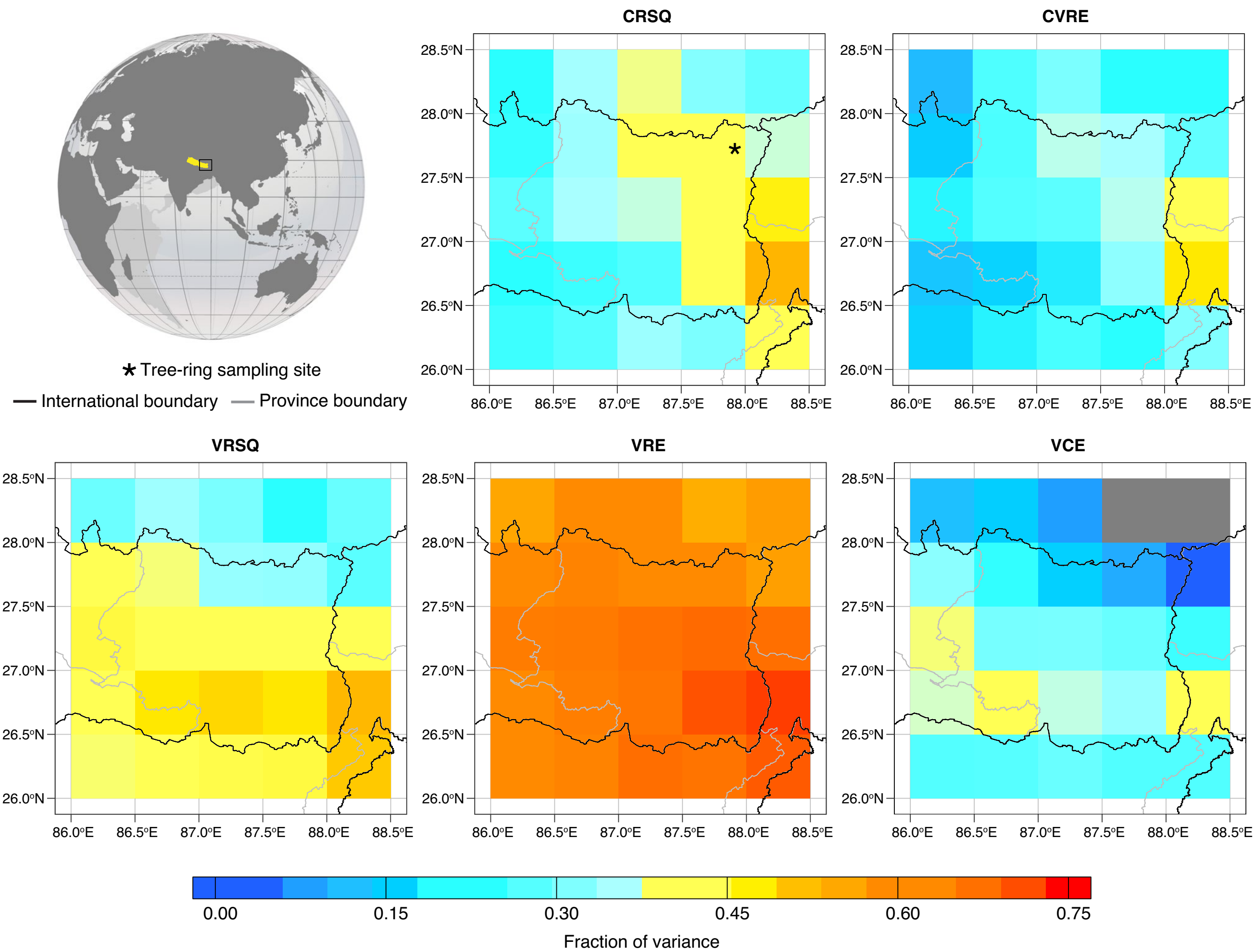

Fig. 5 Calibration and verification statistics for the June–September minimum temperature reconstruction carried out for 25 CRU minimum temperature grid points. Calibrated statistics (prefixed with C) are CRSQ, coefficient of determination; CVRE, cross validation reduction of error, and verification statistic (prefixed with V) are VRSQ, Pearson correlation coefficient squared; VRE, reduction of error statistic; VCE, coefficient of efficiency. All statistics are represented in units of fractional variance. The verification statistic, VCE and VRE plotted only for those grid points with values > 0

Oppenheimer 2003), responsible for cooling much of Northern Hemisphere for a couple of years (Cole-Dai et al. 2009). The $JJAS_{TMN}$ reconstruction suggests that the cooling impacts of these eruptions were also felt in the northeast corner of Nepal. Because our reconstruction is based on ring widths, which are known to have biological memory (Anderegg et al. 2015; Thapa et al. 2017), the longer cooling period following these two eruptions may not represent the true length of volcanic impacts in this region (Esper et al. 2015). Further, our reconstruction, which is based on ring widths that are known to have biological memory, may also be overestimating the length of cooling in the early eighteenth century following eruptions (Esper et al. 2015; Thapa et al. 2017). Wood density measurements from tree-rings are known to be a superior proxy in realistically representing temperature following eruptions, therefore producing new density chronologies might help resolve the issue persisting in reconstruction (Esper et al. 2018).

The power spectral analysis of $JJAS_{TMN}$ reconstruction using Multi Tapered Methods revealed short (2.5) and multidecadal (35, 43, 71 and 100 years) periodicities (Fig. 8). Furthermore, the wavelet analysis showed that the multi-decadal frequency prevails throughout the reconstruction (Fig. 8). The shorter periodicity falls in the frequency cycles of El-Nino Southern Oscillation (ENSO), which is the most dominant climate mode affecting interannual variability of Asian climate, particularly hydroclimate of South Asia (Cook et al. 2010). Such ENSO-like frequency of variability has been reported in several tree-ring–based temperature records across the Himalaya and Tibetan Plateau (Thapa et al 2015; Shah et al. 2019; Aryal et al. 2020a; Gaire et al. 2020, 2022; Huang et al. 2019; Shi et al. 2017), but we observed only a weak correlation

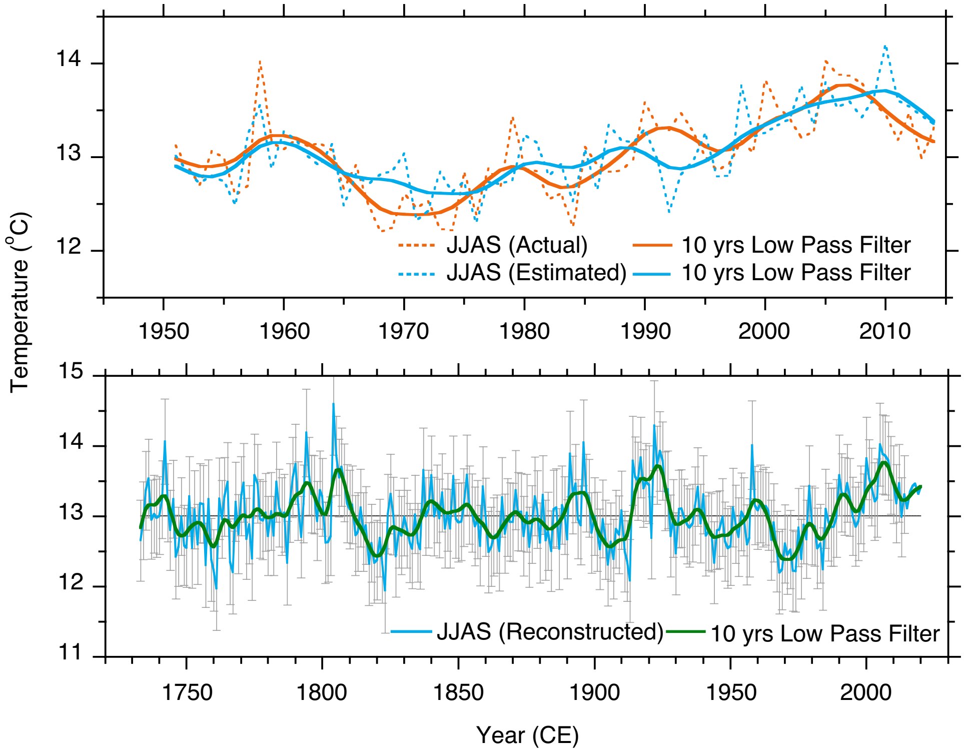

Fig. 6 **a** Actual and estimated June–September minimum temperature for 1951–2014 along with 10 years low pass filter. **b** Reconstructed June–September minimum temperature from 1733 to 2020 CE along with 10 years low pass filter

between our $JJAS_{TMN}$ reconstruction and SSTs over the Nino regions of the tropical Pacific Ocean (Fig. 9). The multidecadal periodicity present in our reconstruction falls in the range of Atlantic Multidecadal Oscillation (AMO; Hurrel et al. 2003), which is also witnessed with highly significant spatial correlation of $JJAS_{TMN}$ reconstruction with SST over the Atlantic region (Fig. 9). This strong positive correlations between our reconstruction and SSTs in the Atlantic Ocean region, suggesting the AMO can have remote influence on the eastern Himalayan temperature variability (Fig. 9).

The previous tree-ring–based reconstructions from the Himalayas and Tibetan plateau have also observed the similar periodicities and indicated the influence of AMO in the climate of the Himalayas and Tibetan Plateau region through atmospheric bridges (Shah et al. 2019; Aryal et al. 2020a; Gaire et al. 2020; Huang et al. 2019; Shi et al. 2017). In a study, St. George (2014) mapped teleconnection patterns associated with major climate modes, over the Northern hemisphere using a network of 2270 tree-ring records, and showed ENSO and the AMO have stronger and more consistent effects on tree growth than do the PDO, PNA, and NAO. Specifically, in Europe and Asia, chronologies are significantly correlated with the AMO index, but the majority of records did not show a strong association with North Atlantic sea-surface temperatures. AMO is a 40–130-year quasi-periodic variation in Atlantic sea-surface temperature (Gray et al. 2004). Simulations with a climate model in the Atlantic Ocean suggested that variability in the Atlantic partially explains the multidecadal variability in the Northern Hemisphere mean temperature record (Zhang et al. 2007). Song et al. (2021) reconstructed winter temperature over Asia for the past 700 years using 260 temperature sensitive tree-ring chronologies. They suggested the possible influence of multidecadal oscillations in regional climate and tree growth along with the influence of volcanic eruptions, anthropogenic activities and winter solar insolation on the winter temperature variations. Shah et al. (2019) in winter temperature reconstruction (1855–2012) for the Lidder Valley, Kashmir, Northwest Himalaya based on tree-rings of *P. wallichiana* found that a significant long-term quasi-periodicity (72 years) may likely be linked to the AMO.

Considering the strong spatial relationship with SSTs in the Atlantic Ocean region, we compared our $JJAS_{TMN}$ reconstruction temporal variations with instrumental and proxy-based AMO records. We found a significant correlation ($r=0.224$, $n=151$, $p<0.05$) between our reconstruction and HadISST1-based AMO index EQ-60N, 0-80W minus SST 60S-60N (Trenberth and Shea 2006). The correlation coefficient increases to 0.312 after applying 10 years of low pass filter (Fig. 10). Similar comparison was made with reconstructed summer Atlantic multidecadal variability (Wang et al. 2017) and annually resolved Atlantic Sea surface temperature variability (Lapointe et al. 2020). In both these comparisons, we observed significant positive correlation and the correlation coefficient increased after applying 10 years of low pass filter (Fig. 10). It was observed that the warm phases of the AMO

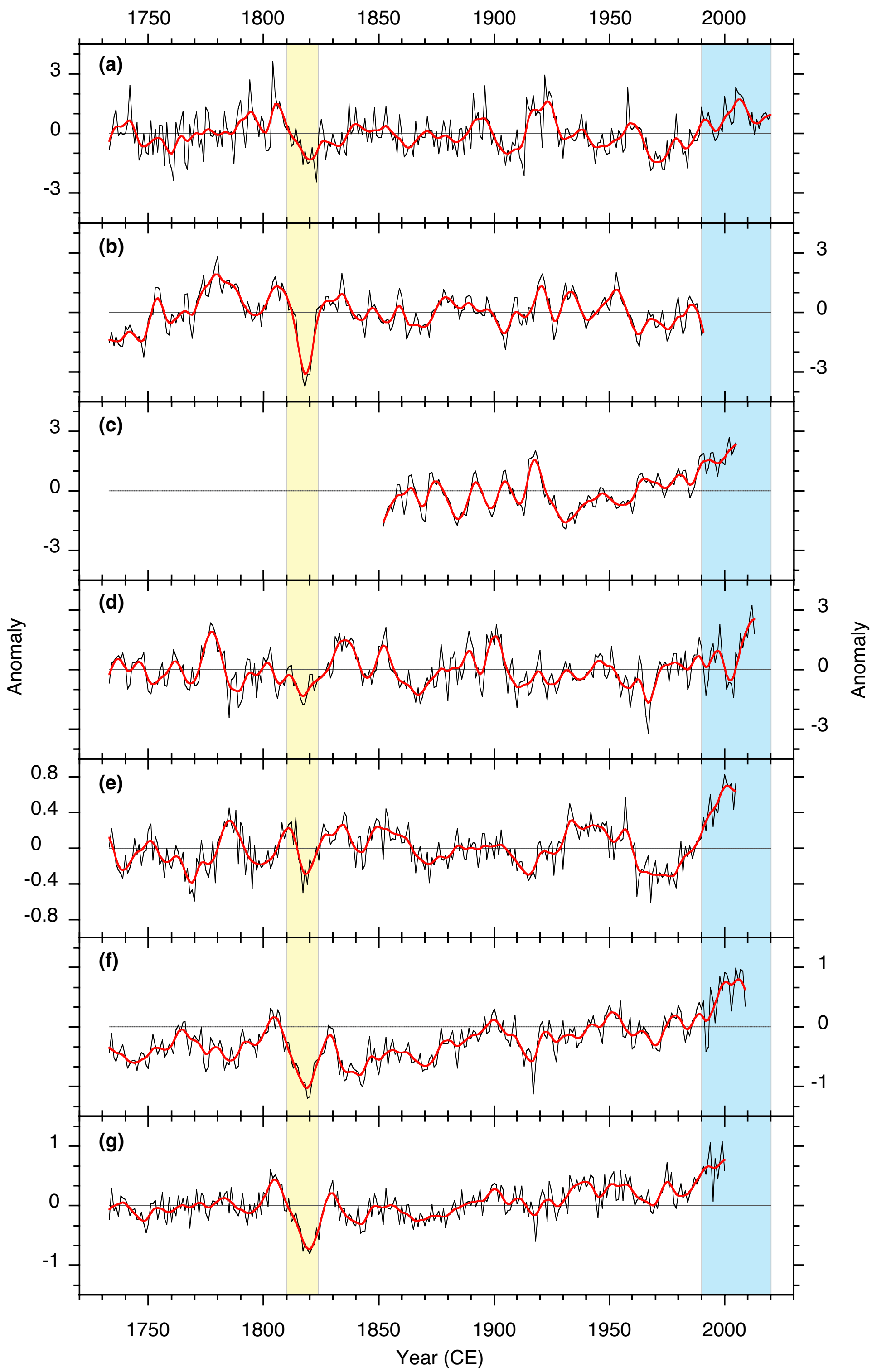

Fig. 7 Comparison of **a** June–September minimum temperature reconstruction from this study with other proxy-based temperature reconstruction, **b** February–June mean temperature, Nepal (Cook et al. 2003), **c** July–September mean temperature from North Sikkim, India (Yadava et al. 2015), **d** June–August mean temperature, Bhutan (Krusic et al. 2015), **e** June–August mean temperature, Eastern Tibetan Plateau (Wang et al. 2015), **f** gridded summer temperature of East Asia (Cook et al. 2013), and **g** Asian summer temperature from PAGES2K Consortium (PAGES2k Consortium 2013). The period with low temperature value due to volcanic eruption of Tambora and recent rise in temperature are highlighted with yellow and blue band respectively

are associated with positive temperature anomalies over the eastern Nepal Himalaya while the cold phase of the AMO is associated with negative temperature anomalies (Fig. 10). This result suggests a close link between the Atlantic Sea surface temperature variability and temperature variations over the eastern Nepal Himalaya at decadal/multidecadal time scales.

4 Conclusions

In this study, we developed an annually resolved robust minimum summer (June–September) temperature back to 1733 CE based on a new *Larix griffithiana* (Sikkim Larch) tree-ring chronology from the eastern Nepal Himalaya. This is

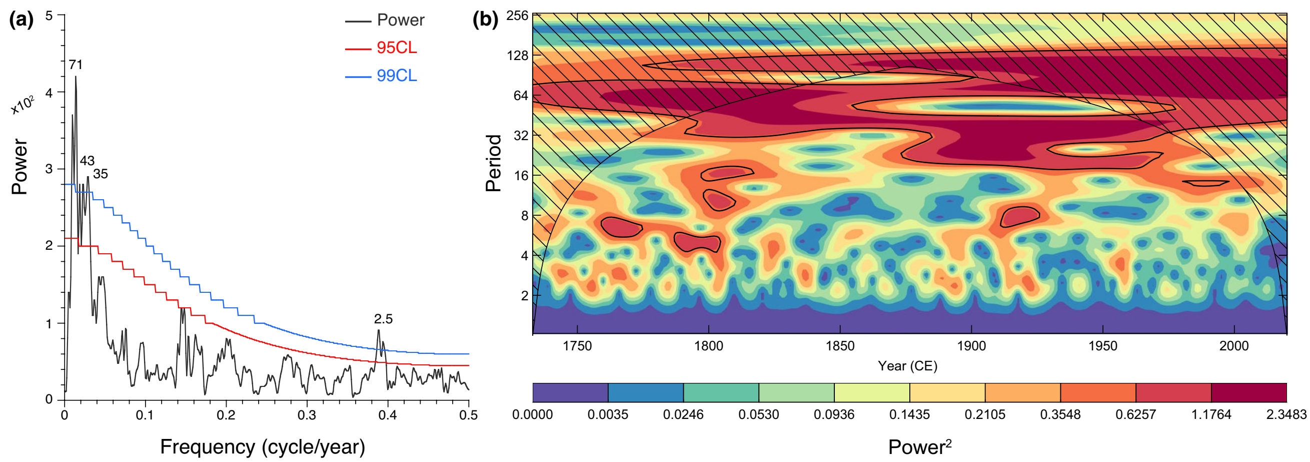

Fig. 8 **a** Multi-tapered power spectral and **b** Morlet's wavelet analysis of the reconstructed June–September minimum temperature from eastern Nepal Himalaya

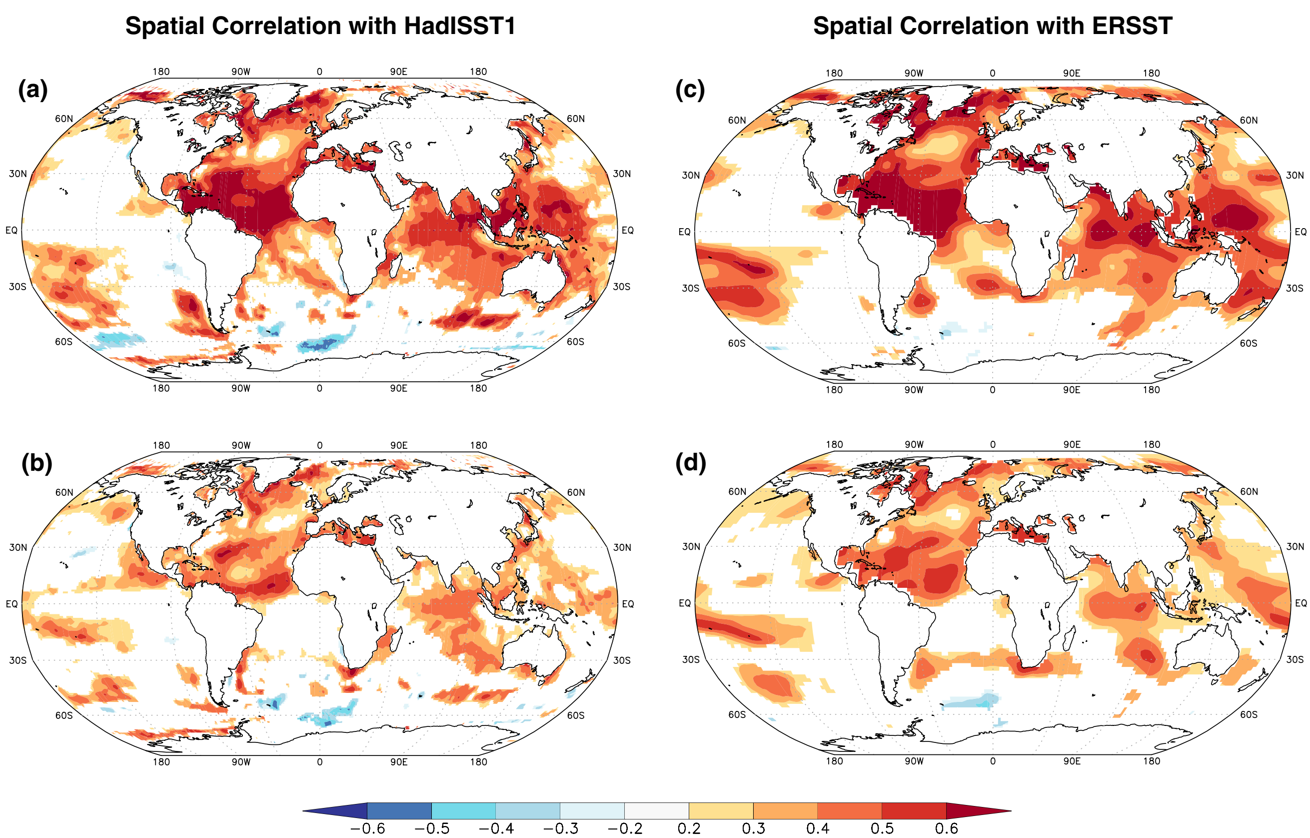

Fig. 9 Spatial correlation between **a** observed June–September temperature and HadISST1, **b** reconstructed June–September temperature and HadISST1, **c** observed June–September temperature and ERRSE v5 and **d** reconstructed June–September temperature and ERRSE v5. All the spatial correlation are calculated for the time period of 1951–2014 CE

a first minimum temperature reconstruction in the eastern Nepal Himalaya that shows that summer warming during the recent decades is unprecedented at least over the past three centuries. The reconstructed temperature series exhibits significant decadal variations, largely driven by the sea surface temperature variability in the Atlantic Ocean region. These findings indicate that it is important to consider the influence of extrinsic factors such as AMO and external forcing factors such as volcanic eruptions in order to improve temperature forecasts in eastern Nepal in the face of anthropogenic climate

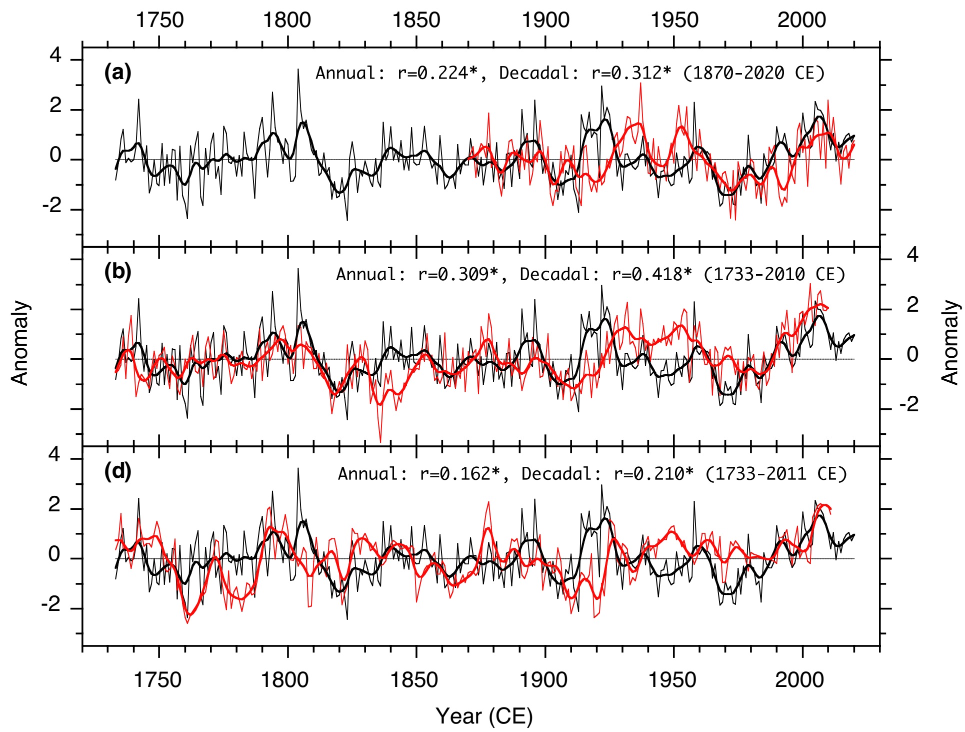

Fig. 10 Comparison of June–September minimum temperature reconstruction from this study with **a** HadISST1 based AMO index EQ-60N, 0-80W minus SST 60S-60N (Trenberth and Shea 2006), **b** reconstructed summer Atlantic multidecadal variability (Wang et al. 2017) and **c** annually resolved Atlantic Sea surface temperature variability (Lapointe et al. 2020). In each graph, correlation between the datasets for both annual and 10-year low pass filter is given in the top right corner

change. Given the difficulty in accessing remote Himalayan forests, our Larix chronology is of great value, and aids in expanding and updating the old collections from the region in the late 1990s. We also acknowledge that our study is based on a single site chronology of *L. griffithiana*. Developing newer tree-ring records and attempting reconstructions based on multiple site chronologies is desirable to increase confidence on regional temperature variability and its drivers.

Acknowledgements The authors are thankful to the Department of National Park and Wildlife Conservation, Kathmandu, Nepal for providing permission to conduct field work in the Kanchanjunga Conservation Area (KCA). The authors also thank the Department of Hydrology and Meteorology, Government of Nepal for providing climate data. The author (SKS) would like to express his gratitude to the Director, Birbal Sahni Institute of Palaeosciences, Lucknow for providing permission to conduct collaborative work with Nepal tree–ring researchers and part of this work is carried out under the Institute In-house Project 6 with permission number (BSIP/RDCC/45/2022-23). The authors are indebted to the anonymous reviewers and editor of the journal for their critical comments and valuable suggestions.

Author contribution Santosh K. Shah, Narayan P. Gaire, and Nivedita Mehrotra: study and worked on conceptualization; methodology; writing, original draft; writing, review and editing. Narayan P. Gaire, Bimal Sharma, Uday Kunwar Thapa, Prakash Chandra Aryal and Dinesh Raj Bhuju: carried out field work to collect tree core samples, processing and dating of the samples. Santosh K. Shah: carried out statistical data analysis and visualization. All authors read and approved the final manuscript and involved in review and editing.

Data availability The reconstructed temperature datasets generated during the current study are available from the corresponding and lead author on reasonable request.

Declarations

Ethics approval and consent to participate This article does not contain any studies with human or animal participants performed by any of the authors. All authors consent to participate in the research.

Consent for publication All authors consent to publish the research findings.

Competing interests The authors declare no competing interests.

References

Allen DM (1974) The relationship between variable selection and data augmentation and a method for prediction. Technometrics 16(1):125–127. https://doi.org/10.1080/00401706.1974.10489157

Anderegg WRL, Schwalm C, Biondi F, Camarero JJ, Koch G, Litvak M, Ogle K, Shaw JD, Shevliakova E, Williams AP, Wolf A, Ziaco E, Pacala S (2015) Pervasive drought legacies in forest ecosystems and their implications for carbon cycle models. Science 349(6247):528–532. https://doi.org/10.1126/science.aab1833

Aryal S, Gaire NP, Pokhrel NR, Rana P, Sharma B, Kharal DK, Poudel BS, Dyola N, Fan Z-X, Grießinger J, Bräuning A (2020a) Spring season in western Nepal Himalaya is not yet warming: a 400-year temperature reconstruction based on tree-ring widths of Himalayan Hemlock (*Tsuga dumosa*). Atmosphere 11:132. https://doi.org/10.3390/atmos11020132

Aryal PC, Dhamala MK, Gaire NP, Bhatta S, Suwal MK, Bhuju DR, Chhetri PK (2020b) Tree-ring climate response of two *Larix* species from the central Nepal Himalaya. Trop Ecol 6:215–225. https://doi.org/10.1007/s42965-020-00082-w

Aryal KP, Kerkhoff EE, Maskey N, Sherchan R (2010) Shifting cultivation in the Sacred Himalayan Landscape. A case study in the Kangchenjunga Conservation Area. WWF Nepal, First Edition. Kathmandu, Nepal

Asahi K, Watanabe T (2000) Past and recent glacier fluctuations in Kanchenjunga Himal. Nepal J Nepal Geol Soc 22:481–490. https://doi.org/10.3126/jngs.v22i0.32419

Bhandari S, Gaire NP, Shah SK, Speer JH, Bhuju DR, Thapa UK (2019) A 307- year tree-ring SPEI reconstruction indicates modern drought in western Nepal Himalayas. Tree Ring Res 75(2):73–85. https://doi.org/10.3959/1536-1098-75.2.73

Bhatta S, Dhamala MK, Aryal PC, Chauhan R, Dawadi B (2018) Climate Variability and Associated Response of Larix Griffithii in Kanchenjunga Conservation Area of Nepal. Appl Ecol Environ Sci 6(1):23–30

Bhattacharyya A, Chaudhary V (2003) Late-summer temperature reconstruction of the Eastern Himalayan Region based on tree-ring data of *Abies densa*. Arct Antarct Alp Res 35(2):196–202. https://doi.org/10.1657/1523-0430(2003)035[0196:LTROTE]2.0.CO;2

Bhattacharyya A, Lamarche VC Jr, Hughes MK (1992) Tree ring chronologies from Nepal. Tree Ring Bull 52:59–66

Bhuju UR, Shakya PR, Basnet TB, Shrestha S (2007) Nepal biodiversity resource book. Protected areas, Ramsar sites, and world heritage sites. International Centre for Integrated Mountain Development (ICIMOD), Kathmandu, Nepal. https://doi.org/10.53055/ICIMOD.475

Bista R, Chhetri PK, Johnson JS, Sinha A, Shrestha KB (2021) Climate-driven differences in growth performance of cohabitant fir and birch in a subalpine forest in Dhorpatan Nepal. Forests 12(9):1137. https://doi.org/10.3390/f12091137

Bolch T, Kulkarni A, Kääb A, Huggel C, Paul F, Cogley JG, Frey H, Kargel JS, Fujita K, Scheel M, Bajracharya S, Stoffel M (2012) The state and fate of Himalayan glaciers. Science 336:310–314. https://doi.org/10.1126/science.1215828

Brooks TM, Mittermeier RA, da Fonseca GAB, Gerlach J, Hoffmann M, Lamoreux JF, Mittermeier CG, Pilgrim JD, Rodrigues ASL (2006) Global biodiversity conservation priorities. Science 313(5783):58–61. https://doi.org/10.1126/science.1127609

Böhner J, Miehe G, Miehe S, Nagy L (2015) Climate and weather. In: Miehe S, Pendry CA, Chaudhary RP (eds) Nepal: an introduction to the natural history, ecology and human environment in the Himalayas, 1st edn. Royal Botanical Garden Edinburgh, London, pp 385–472

Carpenter C, Ghimire S, Brown T (1994) Report on the flora and fauna of the Kanchenjunga Region: wildlands studies. WWF Nepal, Kathmandu, Nepal

Chattopadhyay GP, Dahal DR, Das A (2016) Rapid deglaciation on the Southeast-facing slopes of Kanchenjunga under the present state of global climate change and its impact on the human health in this part of the Sikkim Himalaya. In: Akhtar R (Eds.) Climate change and human health scenario in south and southeast Asia. Advances in Asian Human-Environmental Research. Springer, Cham. https://doi.org/10.1007/978-3-319-23684-1_5

Chaudhary V, Bhattacharyya A (2000) Tree ring analysis of *Larix griffithiana* from the Eastern Himalayas in the reconstruction of past temperature. Curr Sci 79(12):1712–1716

Chaudhary V, Bhattacharyya A (2002) Suitability of *Pinus kesiya* in Shillong, Meghalaya for tree-ring analyses. Curr Sci 83(8):1010–1015

Chaudhary RP, Uprety Y, Joshi SP, Shrestha KK, Basnet KB, Basnet G, Shrestha KR, Bhatta KP, Acharya KP, Chettri N (2015) Kangchenjunga landscape Nepal: from conservation and development perspectives. Ministry of Forests and Science and Technology (MoFSC), Government of Nepal, Kathmandu, Nepal

Chettri N, Sharma E, Shakya B, Thapa R, Bajracharya B, Uddin K, Oli KP, Choudhury D (2010) Biodiversity in the Eastern Himalayas: status, trends and vulnerability to climate change. International Centre for Integrated Mountain Development (ICIMOD), Kathmandu, Nepal

Chhetri PK, Cairns DM (2015) Contemporary and historic population structure of *Abies spectabilis* at treeline in Barun valley, eastern Nepal Himalaya. J Mt Sci 12(3):558–570. https://doi.org/10.1007/s11629-015-3454-5

Cole-Dai J, Mosley-Thompson E, Thompson LG (1997) Annually resolved southern hemisphere volcanic history from two Antarctic ice cores. J Geophys Res 102:761–771. https://doi.org/10.1029/97JD01394

Cole-Dai J, Ferris D, Lanciki A, Savarino J, Baroni M, Thiemens MH (2009) Cold decade (AD 1810–1819) caused by Tambora (1815) and another (1809) stratospheric volcanic eruption. Geophys Res Lett 36:L22703. https://doi.org/10.1029/2009GL040882

Cook ER (1985) A time-series analysis approach to tree-ring standardization. Dissertation, The University of Arizona

Cook ER, Kairiukstis LA (1990) Methods of dendrochronology: applications in the environmental sciences. Kluwer Academic Publishers, Netherlands

Cook ER, Meko DM, Stahle DW, Cleaveland MK (1999) Drought reconstructions for the Continental United States. J Climate 12:1145–1162. https://doi.org/10.1175/1520-0442(1999)012%3c1145:DRFTCU%3e2.0.CO;2

Cook ER, Krusic PJ, Jones PD (2003) Dendroclimatic signals in long tree-ring chronologies from the Himalayas of Nepal. Int J Climatol 23(7):707–732. https://doi.org/10.1002/joc.911

Cook ER, Woodhouse CA, Eakin CM, Meko DM, Stahle DW (2004) Long-term aridity changes in the western United States. Science 306(5698):1015–1018. https://doi.org/10.1126/science.1102586

Cook ER, Anchukaitis KJ, Buckley BM, D'Arrigo RD, Jacoby GC, Wright WE (2010) Asian Monsoon failure and megadrought during the last millennium. Science 328(5977):486–489. https://doi.org/10.1126/science.1185188

Cook ER, Seager R, Kushnir Y et al (2015) Old World megadroughts and pluvials during the Common Era. Sci Adv 1(10):e1500561. https://doi.org/10.1126/sciadv.1500561

Cook ER, Krusic PJ, Anchukaitis KJ, Buckley BM, Nakatsuka T, Sano M (2013) Tree-ringreconstructed summer temperature anomalies for temperate East Asia since 800 C.E. Clim Dyn 41:2957–2972. https://doi.org/10.1007/s00382-012-1611-x

Dhar U (2002) Conservation implications of plant endemism in high-altitude Himalaya. Curr Sci 82(2):141–148

DNPWC (2018) Protected areas of Nepal. Kathmandu, Nepal. https://dnpwc.gov.np/en/. Accessed 1 Oct 2022

Esper J, Schneider L, Smerdon JE, Schone BR, Bungten U (2015) Signals and memory in tree-ring width and density data. Dendrochronologia 35:62–70. https://doi.org/10.1016/j.dendro.2015.07.001

Esper J, St. George S, Anchukaitis K, D'Arrigo RD, Ljungqvist FC, Luterbacher J, Schneider L, Stoffel M, Wilson R, Buntgen U (2018) Large-scale, millennial-length temperature reconstructions from tree-rings. Dendrochronologia 50:81–90. https://doi.org/10.1016/j.dendro.2018.06.001

Fritts HC (1976) Tree rings and climate. Cambridge University Press, Cambridge

Fukui K, Fujii Y, Ageta Y, Asahi K (2007) Changes in the lower limit of mountain permafrost between 1973 and 2004 in the Khumbu Himal, the Nepal Himalayas. Glob Planet Change 55(4):251–256. https://doi.org/10.1016/j.gloplacha.2006.06.002

Gaire NP, Koirala M, Bhuju DR, Borgaonkar HP (2014) Treeline dynamics with climate change at the central Nepal Himalaya. Clim past 10:1277–1290. https://doi.org/10.5194/cp-10-1277-2014

Gaire NP, Bhuju DR, Koirala M, Shah SK, Carrer M, Timilsena R (2017) Tree-ring based spring precipitation reconstruction in western Nepal Himalaya since AD 1840. Dendrochronologia 42:21–30. https://doi.org/10.1016/j.dendro.2016.12.004

Gaire NP, Fan ZX, Shah SK, Thapa UK, Rokaya MB (2020) Tree-ring record of winter temperature from Humla, Karnali, in central Himalaya: a 229 years-long perspective for recent warming trend. Geogr Ann a: Phys Geogr 102(3):297–316. https://doi.org/10.1080/04353676.2020.1751446

Gaire NP, Zaw Z, Fan ZX, Bräuning A, Sharma B, Dhakal YR, Timilsena R, Shah SK, Bhuju DR (2022) Increasing extreme events in the central Himalaya revealed from a tree-ring based multi-century streamflow reconstruction of Karnali River Basin. J. Hydrol 610:127801. https://doi.org/10.1016/j.jhydrol.2022.127801

Gao C, Robock A, Ammann C (2008) Volcanic forcing of climate over the past 1500 years: an improved ice core-based index for climate models. J Geophys Res 113(D23):D23111. https://doi.org/10.1029/2008JD010239

Gray ST, Graumlich LJ, Betancourt JL, Pederson GT (2004) A tree-ring based reconstruction of the Atlantic multidecadal oscillation since 1567 AD. Geophys Res Lett 31:L12205. https://doi.org/10.1029/2004GL019932

Harris I, Osborn TJ, Jones P, Lister D (2020) Version 4 of the CRU TS monthly high-resolution gridded multivariate climate dataset. Sci Data 7:109. https://doi.org/10.1038/s41597-020-0453-3

Holmes RL (1983) Computer-assisted quality control in tree-ring dating and measurement. Tree-Ring Bull 43:69–78

Huang B, Thorne PW, Banzon VF, Boyer T, Chepurin G, Lawrimore JH, Menne MJ, Smith TM, Vose RS, Zhang HM (2017) Extended reconstructed sea surface temperature, Version 5 (ERSSTv5): Upgrades, validations, and intercomparisons. J Clim 30:8179–8205. https://doi.org/10.1175/JCLI-D-16-0836.1

Huang R, Zhu H, Liang E, Liu B, Shi J, Zhang R, Yuan Y, Grießinger J (2019) A tree ring-based winter temperature reconstruction for the southeastern Tibetan Plateau since 1340 CE. Clim Dyn 53(5–6):3221–3233. https://doi.org/10.1007/s00382-019-04695-3

Hurrel JW, Kushnir Y, Ottersen G, Visbeck M (2003). An overview of the North Atlantic Oscillation. Geophysical Monograph Series 134. https://doi.org/10.1029/134GM01

ICIMOD (2015) Bibliography on Kangchenjunga Landscape. International Centre for Integrated Mountain Development, Kathmandu, Nepal. http://lib.icimod.org/record/32610. Accessed 1 Oct 2022

Kandel P, Gurung J, Chettri N, Ning W, Sharma E (2016) Biodiversity research trends and gap analysis from a transboundary landscape, Eastern Himalayas. J Asia-Pac Biodivers 9(1):1–10. https://doi.org/10.1016/j.japb.2015.11.002

Krusic PJ, Cook ER, Dukpa D, Putnam AE, Rupper S, Schaefer J (2015) Six hundred thirty-eight years of summer temperature variability over the Bhutanese Himalaya. Geophys Res Lett 42(8):2988–2994. https://doi.org/10.1002/2015GL063566

Lapointe F, Bradley R, Francus P (2020) Annually resolved Atlantic sea surface temperature variability over the past 2,900 y. PNAS 117(44):27171–27178. https://doi.org/10.1073/pnas.2014166117

Liang E, Dawadi B, Pederson N, Piao S, Zhu H, Sigdel SR, Chen D (2019) Strong link between large tropical volcanic eruptions and severe droughts prior to monsoon in the central Himalayas revealed by tree-ring records. Sci Bull 64(14):1018–1023. https://doi.org/10.1016/j.scib.2019.05.002

Liu B, Liang E, Liu K, Camarero JJ (2018) Species- and elevation-dependent growth responses to climate warming of Mountain forests in the Qinling Mountains. Central China Forests 9(5):248. https://doi.org/10.3390/f9050248

Mann ME, Lees J (1996) Robust estimation of background noise and signal detection in climate time series. Clim Change 33:409–445. https://doi.org/10.1007/BF00142586

Meko DM (1981) Applications of Box-Jenkins methods of time series analysis to the reconstruction of drought from tree rings. Dissertation, The University of Arizona

Melvin TM, Briffa KR (2008) A 'signal-free' approach to dendroclimatic standardisation. Dendrochronologia 26(2):71–86. https://doi.org/10.1016/j.dendro.2007.12.001

Myers N, Mittermeier RA, Mittermeier CG, Da Fonseca GAB, Kent J (2000) Biodiversity hotspots for conservation priorities. Nature 403:853–858. https://doi.org/10.1038/35002501

Olson DM, Dinerstein E (2002) The Global 200: priority ecoregions for global conservation. Ann Mo Bot Gard 89(2):199–224. https://doi.org/10.2307/3298564

Oppenheimer C (2003) Climatic, environmental and human consequences of the largest known historic eruption: Tambora volcano (Indonesia) 1815. Prog Phys Geogr 27(2):230–259. https://doi.org/10.1191/0309133303pp379ra

Ostenfeld CE, Larsen CS (1930) The species of the genus *Larix* and their geographical distribution. Denmark, Luno

Pages 2k Consortium (2013) Continental-scale temperature variability during the past two millennia. Nat Geosci 6(5):339–346. https://doi.org/10.1038/NGEO1797

Panthi S, Fan ZX, Bräuning A (2021) Ring widths of rhododendron shrubs reveal a persistent winter warming in the central Himalaya. Dendrochronologia 65:125799. https://doi.org/10.1016/j.dendro.2020.125799

Rayner NA, Parker DE, Horton EB, Folland CK, Alexander LV, Rowell DP, Kent EC, Kaplan A (2003) Global analyses of sea surface temperature, sea ice, and night marine air temperature since the late nineteenth century. J Geophys Res Atmos 108(D14):4407. https://doi.org/10.1029/2002JD002670

Rinn F (2003) TSAP-Win: time series analysis and presentation for dendrochronology and related applications. Version 0.55 User reference. Heidelberg, Germany

Sahni KC (1990) Gymnosperms of India and adjacent countries. Bishen Singh and Mahendra Pal Singh. Dehradun, India

Sano M, Tshering P, Komori J, Fujita K, Xu C, Nakatsuka T (2013) May–September precipitation in the Bhutan Himalaya since 1743 as reconstructed from tree ring cellulose $\delta^{18}O$. J Geophys Res Atmos 118:8399–8410. https://doi.org/10.1002/jgrd.50664

Shah SK, Bhattacharyya A (2012) Spatio-temporal growth variability three Pinus species of Northeast Himalaya with relation to climate. Dendrochronologia 30(4):266–278. https://doi.org/10.1016/j.dendro.2012.02.003

Shah SK, Mehrotra N (2017) Tree–ring studies of *Toona ciliata* from subtropical wet hill forests of Kalimpong, eastern Himalaya. Dendrochronologia 46:46–55. https://doi.org/10.1016/j.dendro.2017.10.001

Shah SK, Bhattacharyya A, Chaudhary V (2014a) Streamflow reconstruction of Eastern Himalaya River, Lachen "Chhu", North Sikkim, based on tree-ring data of *Larix griffithiana* from Zemu Glacier. Dendrochronologia 32(2):97–106. https://doi.org/10.1016/j.dendro.2014.01.005

Shah SK, Mehrotra N, Bhattacharyya A (2014b) Tree-ring studies from eastern Himalaya: prospects and challenges. Himal Res J II 1:21–28

Shah SK, Pandey U, Mehrotra N, Wiles GC, Chandra R (2019) A winter temperature reconstruction for the Lidder Valley, Kashmir, Northwest Himalaya based on tree-rings of Pinus wallichiana. Clim Dyn 53(7–8):4059–4075. https://doi.org/10.1007/S00382-019-04773-6/FIGURES/10

Sharma E, Chettri N, Tse-ring K, Shrestha AB, Jing F, Mool P, Eriksson M (2010) Climate change impacts and vulnerability in the Eastern Himalayas. International Centre for Integrated Mountain Development (ICIMOD), Kathmandu, Nepal. https://doi.org/10.53055/ICIMOD.497

Shi S, Li J, Shi J, Zhao Y, Huang G (2017) Three centuries of winter temperature change on the southeastern Tibetan Plateau and its relationship with the Atlantic Multidecadal Oscillation. Clim Dyn 49(4):1305–1319. https://doi.org/10.1007/s00382-016-3381-3

Shrestha UB, Gautam S, Bawa KS (2012) Widespread climate change in the Himalayas and associated changes in local ecosystems. PLoS One 7:e36741. https://doi.org/10.1371/journal.pone.0036741

Shrestha AB, Bajracharya SR, Sharma AS, Duo C, Kulkarni A (2017) Observed trends and changes in daily temperature and precipitation extremes over the Koshi river basin 1975–2010. Int J Climatol 37(2):1066–1083. https://doi.org/10.1002/joc.4761

Shrestha AB, Devkota LP (2010) Climate change in the Eastern Himalayas: observed trends and model projections. International Centre for Integrated Mountain Development (ICIMOD), Kathmandu, Nepal

Sigdel SR, Wang Y, Camarero JJ, Zhu H, Liang E, Peñuelas J (2018) Moisture mediated responsiveness of treeline shifts to global warming in the Himalayas. Glob Change Biol 24(11):5549–5559. https://doi.org/10.1111/gcb.14428

Smerdon JE, Cook BI, Cook ER, Seager R (2015) Bridging past and future climate across Paleoclimatic reconstructions, observations, and models: a hydroclimate case study. J Climate 28(8):3212–3231. https://doi.org/10.1175/JCLI-D-14-00417.1

Song M, Yang B, Ljungqvist FC, Shi F, Qin C, Wang J (2021) Tree-ring-based winter temperature reconstruction for East Asia over the past 700 years. Sci China Earth Sci 64:872–889. https://doi.org/10.1007/s11430-020-9768-9

Speer JH (2010) Fundamentals of tree ring research. In The University of Arizona Press. The University of Arizona Press, Tucson, USA

St. George S (2014) An overview of tree-ring width records across the Northern Hemisphere. Quat Sci Rev 95:132–150. https://doi.org/10.1016/j.quascirev.2014.04.029

Stothers RB (1984) The Great Tambora Eruption in 1815 and its aftermath. Science 224:1191–1198. https://doi.org/10.1126/science.224.4654.1191

Sun XB, Ren GY, Shrestha AB, Ren YY, You QL, Zhan YJ, Xu Y, Rajbhandari R (2017) Change in extreme temperature events over the Hindu Kush Himalayan during 1961–2015. Adv Clim Change Res 8(3):157–165. https://doi.org/10.1016/j.accre.2017.07.001

Telwala Y, Brook BW, Manish K, Pandit MK (2013) Climate induced elevational range shifts and increase in plant species richness in a Himalayan biodiversity epicenter. PLoS One 8:e57103. https://doi.org/10.1371/journal.pone.0057103

Thapa UK, Shah SK, Gaire NP, Bhuju DR (2015) Spring temperatures in the far–western Nepal Himalaya since AD 1640 reconstructed from *Picea smithiana* tree–ring widths. Clim Dyn 45:2069–2081. https://doi.org/10.1007/s00382-014-2457-1

Thapa UK, St. George S, Kharal DK, Gaire NP (2017) Tree growth across the Nepal Himalaya during the last four centuries. Prog Phys Geogr: 1–18. https://doi.org/10.1177/0309133317714247

Tiwari A, Fan ZX, Jump AS, Zhou ZK (2017) Warming induced growth decline of Himalayan birch at its lower range edge in a semi-arid region of trans-Himalaya, Central Nepal. Plant Ecol 218:621–633. https://doi.org/10.1007/s11258-017-0716-z

Torrence C, Compo GP (1998) A practical guide to wavelet analysis. Bull Am Meteorol Soc 79:61–78. https://doi.org/10.1175/1520-0477(1998)079%3c0061:APGTWA%3e2.0.CO;2

Trenberth KE, Shea DJ (2006) Atlantic hurricanes and natural variability in 2005. Geophys Res Lett 33:L12704. https://doi.org/10.1029/2006GL026894

Trouet V, Oldenborgh GJV (2013) KNMI climate explorer: a web based research tool for high-resolution paleoclimatology. Tree-Ring Res 69(1):3–13. https://doi.org/10.3959/1536-1098-69.1.3

Wang J, Yang B, Ljungqvist FC (2015) A millennial summer temperature reconstruction for the Eastern Tibetan Plateau from tree-ring width. J Clim 28(13):5289–5304. https://doi.org/10.1175/JCLI-D-14-00738.1

Wang W, Jia M, Wang G, Zhu W, McDowell NG (2017) Rapid warming forces contrasting growth trends of subalpine fir (*Abies fabri*) at higher- and lower-elevations in the eastern Tibetan Plateau. For Ecol Manag 402:135–144. https://doi.org/10.1016/j.foreco.2017.07.043

Wigley TML, Briffa KR, Jones PD (1984) On the average value of correlated time series, with applications in dendroclimatology and hydrometeorology. J Appl Meteorol Climatol 23(2):201–213. https://doi.org/10.1175/1520-0450(1984)023%3c0201:OTAVOC%3e2.0.CO;2

Yadav RR, Park W-K, Singh J, Dubey B (2004) Do the western Himalayas defy global warming? Geophys Res Lett 31:L17201. https://doi.org/10.1029/2004GL020201

Yadava AK, Yadav RR, Misra KG, Singh J, Singh D (2015) Tree ring evidence of late summer warming in Sikkim, northeast India. Quat Int 371:175–180. https://doi.org/10.1016/j.quaint.2014.12.067

Zhan YJ, Ren GY, Shrestha AB, Rajbhandari R, Ren YY, Sanjay J, Xu Y, Sun XB, Lou QL, Wang S (2017) Change in extreme precipitation events over the Hindu Kush Himalayan region during 1961–2012. Adv Clim Change Res 8(3):166–175. https://doi.org/10.1016/j.accre.2017.08.002

Zhang R, Delworth TL, Held IM (2007) Can the Atlantic Ocean drive the observed multidecadal variability in Northern Hemisphere mean temperature? Geophys Res Lett 34(2):L02709. https://doi.org/10.1029/2006GL028683

Zurick D, Pacheco J, Shrestha B, Bajracharya B (2005) Atlas of the Himalaya. International Centre for Integrated Mountain Development (ICIMOD), Kathmandu, Nepal

Publisher's note Springer Nature remains neutral with regard to jurisdictional claims in published maps and institutional affiliations.

Springer Nature or its licensor (e.g. a society or other partner) holds exclusive rights to this article under a publishing agreement with the author(s) or other rightsholder(s); author self-archiving of the accepted manuscript version of this article is solely governed by the terms of such publishing agreement and applicable law.